Stacking faults in $YBa_2Cu_3O_{7-x}$: Measurement using x-ray diffraction and effects on critical current

E. D. Specht,[a] A. Goyal, J. Li, and P. M. Martin
Oak Ridge National Laboratory, Oak Ridge, Tennessee 37831

X. Li and M. W. Rupich
American Superconductor Corporation, Westborough, Massachusetts 01581

(Received 15 August 2006; accepted 4 September 2006; published online 18 October 2006)

The density n of stacking faults (SFs) in epitaxial $YBa_2Cu_3O_{7-x}$ (Y123) films, consisting of extra CuO planes, is measured by fitting x-ray diffraction patterns using a random stacking model. The SF density is $n=0.068\ \mathrm{nm}^{-1}$ in films grown by metal-organic deposition on textured templates and optimized for high I_c. The presence of SF is correlated with pinning of magnetic field (H) applied in the Y123 *ab* plane. SF can be nearly eliminated by a high temperature anneal, or by adding excess Dy, resulting in I_c which is nearly independent of the orientation of H. © *2006 American Institute of Physics*. [DOI: 10.1063/1.2364185]

Epitaxial $YBa_2Cu_3O_{7-x}$ (Y123) thin films can support high I_c when the magnetic field vortices are pinned; however, the responsible pinning mechanisms have not been clearly identified. Improved understanding and control of these pinning mechanisms will aid in the development of films for high-I_c applications. Possible pinning mechanisms include the Y123 lattice (intrinsic pinning)[1] and naturally formed lattice defects such as precipitates,[2] twins,[3] grain boundaries,[3] edge dislocations,[4] screw dislocations,[5] and stacking faults (SFs).[6]

SFs are of particular interest because they appear to be an important pinning mechanism for *ex situ* Y123 films prepared from BaF_2 precusors.[6] Such films, important for potential high-current applications, are grown in two steps: a precursor film is first deposited, then chemically converted to Y123.[7] The *c*-axis stacking sequence of defect-free, fully oxygenated Y123 is $BaO-CuO_2-Y-CuO_2-BaO-CuO$.[8] The SFs which occur in *ex situ* Y123 films are believed to consist of an extra CuO plane: $BaO-CuO_2-Y-CuO_2-BaO-CuO-CuO$.[6] The $YBa_2Cu_4O_8$ (Y124) structure corresponds to such a SF in every Y123 cell,[9] while the $Y_2Ba_4Cu_7O_{15}$ structure corresponds to SF in alternate Y123 cells.[10]

This letter is concerned with measuring SF density n in epitaxial Y123 films and the correlation between SF and the value of I_c when H is in the *ab* plane of the Y123 films. SF are generally measured using transmission electron microscopy (TEM);[6,11–15] however, sample preparation is time consuming and destructive. In addition, only a small portion of the sample can be examined, so the results may not be representative of the entire sample. We demonstrate that analysis of x-ray diffraction (XRD) line broadening can be used to provide a rapid, quantitative, nondestructive measure of n over a large area of the film.

All samples were prepared on rolling assisted biaxially textured substrates[16] (RABiTS™) with the configuration Ni–5 at.% W (75 μm)/Y_2O_3 (75 nm)/YSZ (75 nm)/CeO_2 (75 nm). Details of substrate fabrication and characterization have been reported elsewhere.[17] Y123 and Dy-doped Y123 films were prepared using a metal-organic deposition (MOD) process. Films were reacted at ~750 °C in a humidified, low-O_2 atmosphere, cooled to ambient temperature and then oxygenated at <600 °C to form the orthorhombic phase. Complete details of processing parameters and conditions have been reported elsewhere.[18] Selected Y123 films were given an additional high temperature oxygen anneal (HTOA) at 750–750 °C in 500 ppm O_2 after the reaction step, then oxygenated at <600 °C to form the orthorhombic phase.

I_c was measured by transport using a standard four-point probe method with a voltage criterion of 1 μV/cm. The angular dependence of I_c was measured at 77 K with H applied in the maximum Lorentz force configuration, perpendicular to the current. Transmission electron microscopy (TEM) was carried out using a Hitachi HF-2000 and a Philips CM200 microscope, both using a field emission gun operated at 200 kV. XRD measurements were made using a standard Rigaku diffractometer with Cu $K\alpha$ radiation.

For (001)-textured films, only (00l) XRD peaks are observed for Y123; peaks from the substrate and buffer layers are ignored. After annealing, the Y123 peaks are well described by a Lorentzian-squared line shape:

$$L(2\theta) = A[1 + (2\theta - 2\theta_L)^2/\kappa^2]^{-2}, \tag{1}$$

where the full width at half maximum (FWHM) $\Delta 2\theta = 1.29\kappa$ follows the form expected for an inhomogeneous strain:

$$\Delta 2\theta_L = 2\varepsilon \tan \theta_L, \tag{2}$$

where $\varepsilon = 0.0038$ is the FWHM of the strain distribution. In this case, the inhomogeneous strain is likely due to an oxygen stoichiometry gradient through the thickness of the film.

The diffracted intensity $F(2\theta)$ from a crystal with SF is given by Eq. (20) of Hendricks and Teller.[19] This model assumes that the structure consists of a random sequence of 1.361 nm Y124 layers occurring with probability f_{124} and 1.168 nm Y123 layers occurring with probability $f_{123} = 1 - f_{124}$. The bulk structures of Y123 and Y124 are used to find the scattering factors of each layer.[8,9] Each peak is modeled by a numerical convolution of the diffracted intensity F from an ideal randomly faulted crystal with the peak profile L

[a]Author to whom correspondence should be addressed; electronic mail: spechted@ornl.gov

 © 2006 American Institute of Physics
Downloaded 06 Sep 2009 to 160.91.157.167. Redistribution subject to AIP license or copyright; see http://apl.aip.org/apl/copyright.jsp

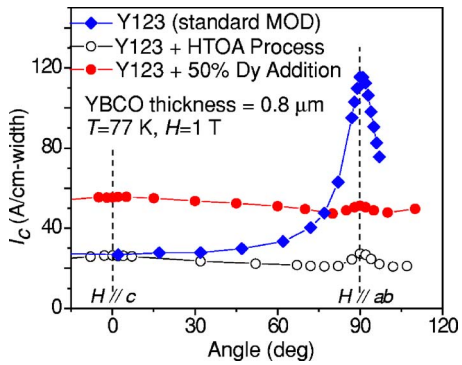

FIG. 1. (Color online) Dependence of I_c on the orientation of H (1 T, 77 K): Y123 prepared with the standard MOD process (♦); Y123 film with HTOA (○); and Dy-doped Y123 (●). Calculated Y123 thickness is 0.8 μm.

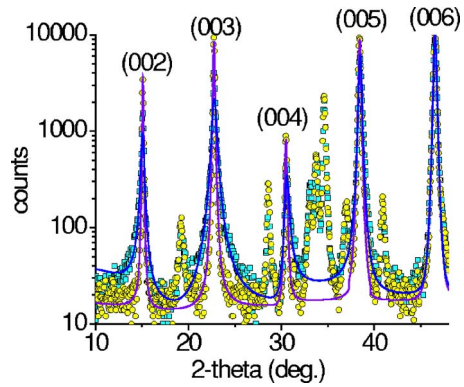

FIG. 2. (Color online) XRD scans and fit for Y123 films: standard MOD processing (■) modeled with f_{124}=0.08 (upper line); after HTOA film (○) modeled with f_{124}=0.01 (lower line). Unindexed peaks are due to substrate and buffer layers.

from a real, unfaulted film which is broadened due to instrumental effects and lattice parameter variation:

$$I(2\theta) = \frac{1+\cos^2\theta}{\sin^2\theta\cos\theta}\int_{-8\kappa}^{8\kappa} L(x)F(2\theta+x)dx, \quad (3)$$

where the first term is the Lorentz-polarization factor for powder diffraction,[20] and L is given in Eq. (1). A linear background is added. Each pattern is fit by varying the intensity A of each peak, the probability f_{124} of SF, and the slope and intercept of the background; the widths κ are fixed from analysis of an annealed sample.

Because six Y124 layers are equal in thickness to seven Y123 layers to within 0.12%, the Y123 (006) reflection is not significantly broadened by faulting, and the convolution of Eq. (3) becomes difficult to perform. The (006) peak is modeled by a Lorentzian-squared line shape [Eq. (1)], as are the unfaulted films. The lack of broadening of the (006) reflection is characteristic of Y124-type SF and supports the conclusion that this is the dominant SF in these films.

MOD Y123 films on RABiTS™ typically display a strong peak in the angular dependence of I_c on H at 77 K for $H \| ab$ plane[18] (Fig. 1, ♦). However, I_c for this field alignment drops dramatically in samples given the HTOA step, while there is no measurable change in the I_c with the field oriented along the c axis (Fig. 1, ○). These data indicate that the pinning centers responsible for the high currents for $H \| ab$ plane are eliminated by the high temperature annealing.

XRD analysis (Fig. 2, ■) of the Y123 sample prepared with the standard process shows the presence of numerous 124-type defects with the best fitting model of f_{124}=0.08 (upper line) (n=0.068 nm^{-1}). The identity of the defects as 124-type SF is supported by detailed agreement between

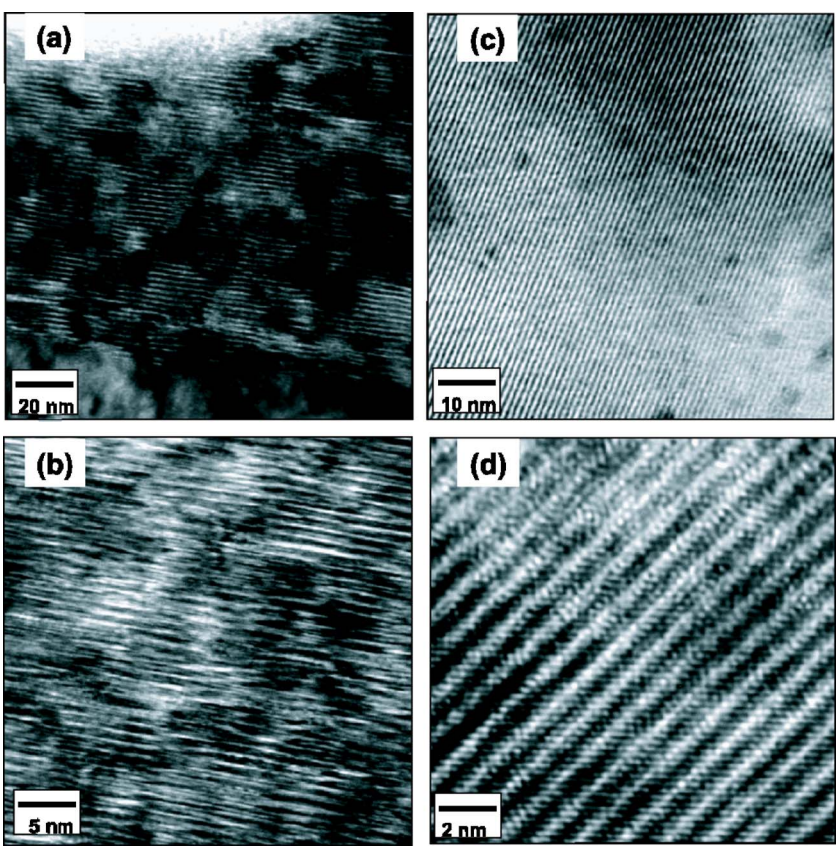

FIG. 3. (Color online) TEM images: [(a) and (b)] standard MOD processing of Y123, showing a high density of 124-type SF; no faulting is apparent (c) after HTOA or (d) with 50% excess Dy.

Downloaded 06 Sep 2009 to 160.91.157.167. Redistribution subject to AIP license or copyright; see http://apl.aip.org/apl/copyright.jsp

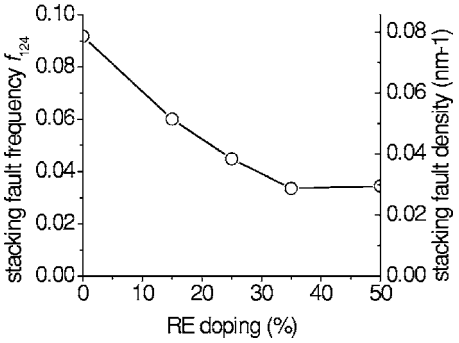

FIG. 4. SF probability and density for Y123 films doped with excess Dy.

model and observations: the (006) reflection exhibits no broadening beyond that of the unfaulted sample, and the other peaks have characteristic asymmetries. The (002) reflection is broadened more on the lower-angle side, the (003) on the higher angle. TEM analysis of a similar sample [Figs. 3(a) and 3(b)] confirms the presence of the 124-type SF. In contrast, XRD analysis of a sample after the HTOA process (Fig. 2, ○) shows that the best fit is for $f_{124}=0.01$ (lower line) ($n=0.086\ \mathrm{nm}^{-1}$), indicating that almost no SFs are present, which was confirmed by TEM [Fig. 3(c)]. These results suggest that the enhanced *ab*-plane pinning is due to the presence of the 124 SF.

The addition of excess rare earth (RE) atoms into the Y123 films also reduces the I_c peak for H oriented in the *ab* plane. Figure 1 (●) shows results for a sample containing a 50% Dy addition. This effect is similar to that resulting from the HTOA process; however, the addition of Dy also increases the pinning in perpendicular field orientations as indicated by the broad peak for $H\|c$ compared to the undoped Y123 sample. TEM confirms that RE doping greatly reduces n as shown in Fig. 3(d) for a sample with 50% excess Dy doping.

XRD analysis of Dy-doped Y123 films in Fig. 4 shows that the SF frequency decreases with increasing RE concentration, with the effect saturating at $f_{124}=0.03$ ($n=0.026\ \mathrm{nm}^{-1}$) for doping beyond 30%. The Dy-free sample in Fig. 4 was prepared similarly to the sample used in Fig. 3, but has a slightly different n.

The enhanced I_c observed for $H\|ab$ in the MOD-based Y123 films is associated with the presence and density of 124-type SF. Small changes in the processing parameters of the MOD-based Y123 films, such as insertion of the HTOA step or the addition of excess RE atoms, can drastically alter the Y124-type SF density and thus I_c for $H\|ab$. The development of a commercial process for preparing Y123 films for superconducting wire applications requires the ability to reproducibly control the density of SF in order to tune the performance of the Y123 films for optimized performance as a function of applied magnetic field and field orientation.

In conclusion, in order to facilitate the development of the optimum parameters and to assist in establishing the mechanism for the 124-type SF growth, a simple XRD analysis was developed to measure the 124-type SF density in Y123 films prepared by the MOD process. The identity of the defects is confirmed by characteristic asymmetries in peak broadening which are seen to agree in both observed and calculated diffraction patterns, as well as the absence of broadening in the (006) reflection. This simple XRD technique provides a rapid means of optimizing processing parameters to adjust the 124 SF density in the Y124 films. The XRD and TEM characterizations are complementary: XRD is most sensitive to high densities of SF, where TEM images become unclear, while SFs are best resolved using TEM at low SF densities, where XRD patterns become difficult to distinguish from those of unfaulted samples. Future work will address conditions under which SFs form and are removed.

The fitting of XRD data provides a rapid, nondestructive, quantitative measure of the 124-type SF density in Y123 films which is correlated to the strong peak in the angular dependence of I_c at 77 K for $H\|ab$. The pattern of peak broadening observed in the XRD scans is specific to the crystallography of the 124-type SF. The 124-type SF densities can be measured down to a 1% frequency or a density of $0.009\ \mathrm{nm}^{-1}$. The method described in this letter to estimate the SF density provides a convenient and expedient, nondestructive way of determining the SF density and hence enables optimization of transport properties of Y123 films in 2G HTS wires.

This research was sponsored by the United States Department of Energy, Office of Science, Basic Energy Sciences, Office of Electricity Delivery and Energy Reliability, Superconductivity Program for Electric Power Systems, and performed at the Oak Ridge National Laboratory under Contract No. DE-AC05-00OR22725 with UT-Battelle, LLC.

[1] M. Tachiki and S. Takahashi, Solid State Commun. **72**, 1083 (1989).
[2] M. Murakami, M. Morita, K. Doi, and K. Miyamoto, Jpn. J. Appl. Phys., Part 1 **28**, 1189 (1989).
[3] P. H. Kes, A. Pruymboom, J. Vandenberg, and J. A. Mydosh, Cryogenics **29**, 228 (1989).
[4] A. Diaz, L. Mechin, P. Berghuis, and J. E. Evetts, Phys. Rev. Lett. **80**, 3855 (1998).
[5] J. Mannhart, D. Anselmetti, J. G. Bednorz, A. Catana, C. Gerber, K. A. Muller, and D. G. Schlom, Z. Phys. B: Condens. Matter **86**, 177 (1992).
[6] P. C. McIntyre and M. J. Cima, J. Mater. Res. **9**, 2778 (1994).
[7] X. Li, M. W. Rupich, W. Zhang, N. Nguyen, T. Kodenkandath, U. Schoop, D. T. Verebelyi, C. Thieme, M. Jowett, P. N. Arendt, S. R. Foltyn, T. G. Holesinger, T. Aytug, D. K. Christen, and M. P. Paranthaman, Physica C **390**, 249 (2003).
[8] T. Siegrist, S. Sunshine, D. W. Murphy, R. J. Cava, and S. M. Zahurak, Phys. Rev. B **35**, 7137 (1987).
[9] P. Marsh, R. M. Fleming, M. L. Mandich, A. M. DeSantolo, J. Kwo, M. Hong, and L. J. Martinez-Miranda, Nature (London) **334**, 141 (1988).
[10] J. Karpinski, E. Kaldis, S. Rusiecki, E. Jilek, P. Fischer, P. Bordet, C. Chaillout, J. Chenavas, J. L. Hodeau, and M. Marezio, J. Less-Common Met. **150**, 129 (1989).
[11] H. W. Zandbergen, R. Gronsky, K. Wang, and G. Thomas, Nature (London) **331**, 596 (1988).
[12] A. Ourmazd, J. A. Rentschler, J. C. H. Spence, M. O'Keeffe, R. J. Graham, D. W. Johnson, and W. W. Rhodes, Nature (London) **327**, 308 (1987).
[13] C. Grigis, S. Schamm, and D. Dorignac, J. Mater. Res. **14**, 2732 (1999).
[14] J. W. Seo, B. Kabius, C. L. Jia, H. Soltner, U. Poppe, and K. Urban, Physica C **225**, 158 (1994).
[15] C. L. Jia, H. Soltner, B. Kabius, U. Poppe, K. Urban, and J. Schubert, Physica C **182**, 163 (1991).
[16] A. Goyal, D. P. Norton, J. D. Budai, M. Paranthaman, E. D. Specht, D. M. Kroeger, D. K. Christen, Q. He, B. Saffian, F. A. List, D. F. Lee, P. M. Martin, C. E. Klabunde, E. Hartfield, and V. K. Sikka, Appl. Phys. Lett. **69**, 1795 (1996).
[17] A. Goyal, M. P. Paranthaman, and U. Schoop, MRS Bull. **29**, 552 (2004).
[18] M. W. Rupich, D. T. Verebelyi, W. Zhang, T. Kodenkandath, and X. P. Li, MRS Bull. **29**, 572 (2004).
[19] S. Hendricks and E. Teller, J. Chem. Phys. **10**, 147 (1942).
[20] B. D. Cullity and Stuart R. Stock, *Elements of X-ray Diffraction*, 3rd ed. (Prentice Hall, Upper Saddle River, NJ, 2001), p. 149.

Downloaded 06 Sep 2009 to 160.91.157.167. Redistribution subject to AIP license or copyright; see http://apl.aip.org/apl/copyright.jsp